Partial Discharge Characteristics of Winding Wires Utilizing the Cellular Coating

Daisuke Muto[*1], *Keisuke Ikeda*[*1], *Keiichi Tomizawa*[*1]
Hideo Fukuda[*2], *Masahiro Kozako*[*3], *Masayuki Hikita*[*3]

ABSTRACT Since the design of motors of the xEV (electric cars) has been accelerating to be smaller in their size and larger in their output power to improve the driving performance and the fuel efficiency, the winding wire applied to the motors is required to have an insulating coating with a higher insulation performance. Furukawa Electric investigated to improve the Partial Discharge Inception Voltage (PDIV) and developed the insulation with a remarkably enhanced PDIV and a low permittivity by introducing micro cavities into the insulation coating. We tested the influence of the mechanical stress and the wave form of the applied voltage on the partial discharge performance of the winding wire utilizing the enamel coating containing micro cavities. When the wire was elongated on the assumption that the wire was winding during coil manufacturing, it was demonstrated that the PDIV kept a proper performance, according to the result. When the impulse voltage was applied, the PDIV was higher compared to the application of the utility alternating current frequency and the phenomenon was explained by the Volume-Time theory.

1. INTRODUCTION

Recently, due to environmental regulation conditions of individual countries, such as the demand to reduce the CO_2 emission, the driving motors being integrated in vehicles, such as hybrid electric vehicles (HEV) and electric vehicles (EV) are rapidly growing. A driving motor is a very important component directly influencing the driving performance and the fuel efficiency, which works not only as a driving power source but also works as a generator during deceleration to charge a battery. The motor is required to improve its output level despite a size reduction and its higher performance. The situation requires further that a high operating voltage over 400V is applied to meet the demand of a higher torque performance. In general, an inverter is integrated in a vehicle, which in turn can control the rotational speed with precision. However, a problem is observed that the coil insulation is damaged when subjected to a high voltage surge with a steep rise generated from the high speed switching of the inverter (that is the inverter surge).

We have started to work on an R&D on the partial discharge phenomenon and the damaged insulation caused by the inverter surge very early even in the winding wire industry. And as the result of our best effort to determine the mechanism and to improve the PDIV for the enameled coating of the winding wire, we were the first succeeding in the development of the High Voltage Winding Wire (HVWW) worldwide[1]. And furthermore, in order to improve the partial discharge performance of the enameled coating, we have succeeded in the development of the low permittivity insulation material by introducing micro cellular coating into the enameled coating, which has extremely improved the PDIV[2]. In this paper, we report that the influence of the mechanical stress and the wave form of the applied voltage on the partial discharge performance of the winding wire utilizing the enameled micro cellular coating[3)-5)].

2. LOW PERMITTIVITY OF THE ENAMEL COATING INSULATION INTRODUCING MICRO CELLULAR COATING

Aiming at the improvement of the resistive characteristics against the partial discharge, we have been working on lowering the permittivity of the insulation coating by introducing air into the enameled resin, and we have succeeded in the development of the enameled wire with an enameled insulation containing fine micro cellular coating (the winding wire with micro cellular coating) based on our newly developed original composite of enameled resin. A sketch of the developed winding wire is shown in

[*1] Automotive Products & Electronics Laboratories,R&D Division
[*2] FURUKAWA MAGNET WIRE CO., LTD., Technical Division
[*3] Kyushu Institute of Technology

Figure 1. Applying the developed composite, the relative permittivity of the insulation coating is able to be drastically reduced in comparison with the conventional enameled wire, and also excellent PDIV performance is realized by increasing the thickness of the enameled coating. The result of PDIV measurement at 25 °C for the micro cellular coating containing the winding wire, whose cellular coating against the enameled coating is 40% in volume ratio is shown in Figure 2. The result of the conventional winding wire without micro cellular coating is also shown in the same figure for comparison.

Since the electric field enhancement in the air gap between the winding wires is reduced using the micro cellular enameled winding wire, the partial discharge from the inverter surge can be prevented.

3. THE INFLUENCE OF THE MECHANICAL STRESS ON THE PDIV OF THE CELLULAR ENAMELED WINDING WIRE

Along with the size reduction of motors for cars, more severe manufacturing is applied on the winding wire. It is important to clarify the influence of the mechanical stress, such as elongation, bending, etc., on the partial discharge performance of the winding wire. The PDIV performance for elongated twist paired winding wires with micro cellular enameled insulation is mentioned in this chapter[3].

3.1 Experiment

3.1.1 Twisted pair sample

The sample for the experiment was the winding wire with cellular insulation (cellular wire) of polyamide imide (PAI) enameled layer containing micro cellular coating with an average diameter of 2 μm.

The structure of the specimen was the twisted pair wire as shown in Figure 3. The PAI enameled winding wire without micro cellular coating (non-cellular wire) was also measured for comparison. The permittivity of the cellular coated wire and the non-cellular coated wire were 2.7 and 4.2 respectively, and the thickness of the enameled coated were 39μm and 40μm respectively. The conductor diameter of both specimens is 1.0 mm. In order to simulate the mechanical stress on the wire, the wires were elongated at constant speed in longitudinal direction and the twisted pair specimens were prepared using the wires at 10%, 20% and 30% of the elongation rate. The elongation rate ϕ is shown in the following equation (1).

$$\phi = \frac{(L_f - L_0)}{L_0} \times 100\,[\%] \qquad (1)$$

L_0 is the gage length and L_f is the gage length after elongation. Hereafter the cellular coating and the non-cellular coating twisted pair specimens are abbreviated the cellular specimen and the non-cellular specimen respectively.

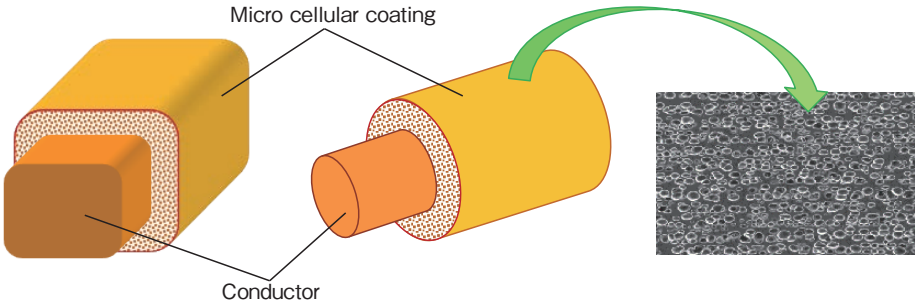

Figure 1 Schematic diagram of the developed winding wires coated with the micro cellular coating.

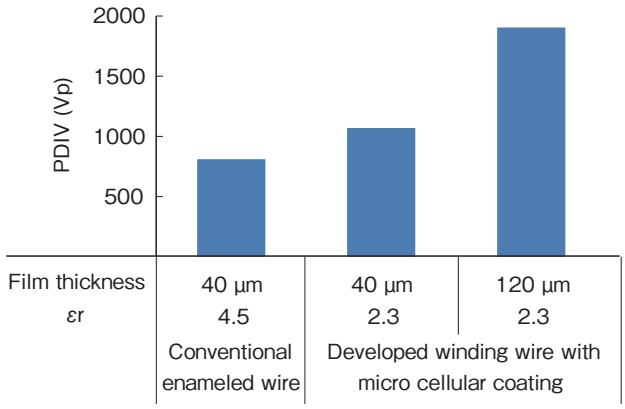

Figure 2 Comparison of PDIV between the conventional enameled wire and the developed micro cellular enameled winding wire.

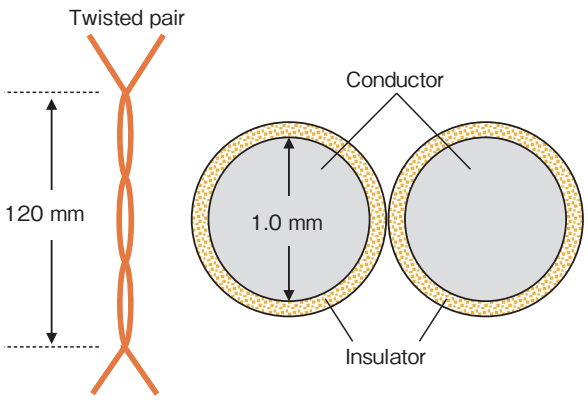

Figure 3 Structure of the specimen.

3.1.2 Partial discharge inception voltage (PDIV)

The measurement circuit of the partial discharge is shown in Figure 4. The alternative current (60 Hz) at a rise rate of 50 V/s was applied to the specimen and the PDIV was measured using the partial discharge measuring device (NIHON KEISOKUKI SEIZOSHO CO., LTD., TYPE CD-6) with a sensitivity of 2.3 pC. The crest value of the charged voltage was determined as the PDIV value. The PDIV was repeatedly measured 12 times on the sample. Deleting of the maximum value and the minimum value among twelve data and the average value of the other data was evaluated. The number of each specimen was 3.

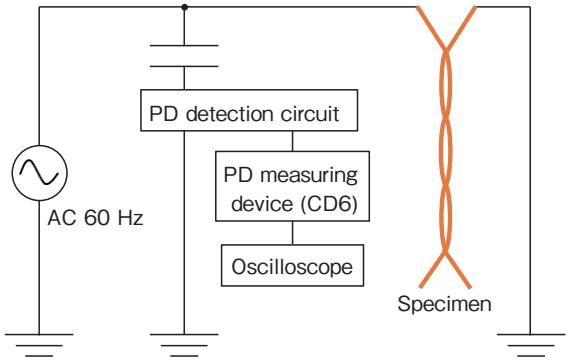

Figure 4 Measurement circuit of the partial discharge under alternate current voltage.

3.1.3 Relative permittivity

The conductive paint was applied on the coating insulation surface of the cellular wire and the non-cellular wire, and the capacitance *C* of the total coating insulation was measured. According to the measurement result, the relative permittivity ε_r of the total coating was calculated using the equation (2) for the coaxial cylindrical capacitance. Measurement frequency was 100 Hz and measurement temperature was 25 °C. In the equation (2), l is the electrode length, *a* and *b* are the inner diameter and the outer diameter of the coaxial cylinder respectively.

$$C = \frac{2\pi\varepsilon_0\varepsilon_r l}{\ln\frac{b}{a}} \quad (2)$$

3.2 Experiment Result and Discussion

3.2.1 The partial discharge experiment result for the elongated twisted pair specimen

The PDIV measurement result of the twisted pair specimens with elongation rates from 10% to 30% is shown in Figure 5. Both specimens showed that the PDIV decreased with the increase of the elongation rate. The result suggests that the PDIV decreased due to the decrease of the enameled coating thickness *t* and increasing the relative permittivity ε_r based on Dakin's estimated equation (3) for the PDIV.

$$V = 163\left(\frac{t}{\varepsilon_r}\right)^{0.46} \quad (3)$$

The PDIV value of the cellular specimen was 18% to 26% higher than the non-cellular specimen at elongation rates from 10% to 30%. The result suggested that the cellular wire with 30% of elongation maintained low permittivity. We investigated the reason of the decreasing of the PDIV due to the elongation from the view point of the enameled coating thickness *t* and the relative permittivity ε_r in chapters 3.2.2 and 3.2.3.

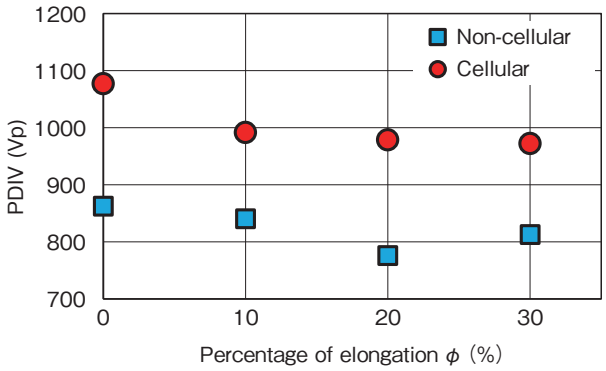

Figure 5 The relationship between the PDIV and elongation rates.

3.2.2 Enameled coating thickness

Figure 6 shows the change of the coating thickness due to the elongation rate. According to Figure 6, the thickness of the cellular and the non-cellular specimens decreased the enameled coating thickness with the increase of the elongation rate, and when both types of twisted pair specimens were elongated at 30%, the thickness decreased 8.8 % and 11 % for each of the specimens respectively.

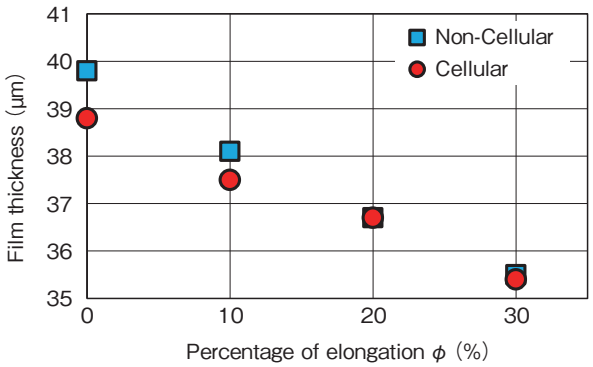

Figure 6 The relationship between the thickness and the elongation rate.

3.2.3 Relative permittivity

The measurement result of the relative permittivity with the change of the elongation rate is shown in Figure 7. The permittivity of the non-cellular specimen kept a constant value when the coating thickness is getting thinner, but the cellular specimen decreased by 3 % of its permittivity when the coating thickness is getting thinner. According to the result, it is assumed that the capaci-

tance of the total coating decreased since the cellular shape has changed with the coating thickness getting thinner[3].

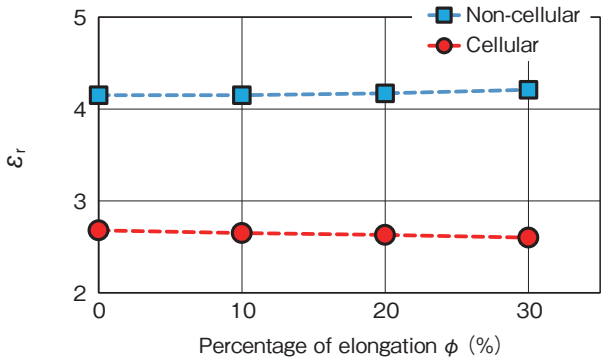

Figure 7 The relationship between the relative permittivity and the elongation rate.

The result suggests that the reason of PDIV decreasing with the increase of the elongation is due to the decrease of the enameled coating thickness.

3.2.4 Estimation of the PDIV by the electric field calculation and Paschen's law

An attempt was made to estimate the PDIV under assumption that PD occurs in the air wedge gap between enameled cellular wires when applying the AC voltage from the electric field distribution calculation and the Paschen's law. Using the numerical electric field analysis software of Electro of Integrated Engineering Software Inc., the analysis model for the twisted pair was made and shown in Figure 8. The electric field simulation was made to obtain the electric field E with respect to each gap length d of the wedge gap for a predetermined electric potential V_a applied between winding wires, and the electric fields versus each gap length were plotted.

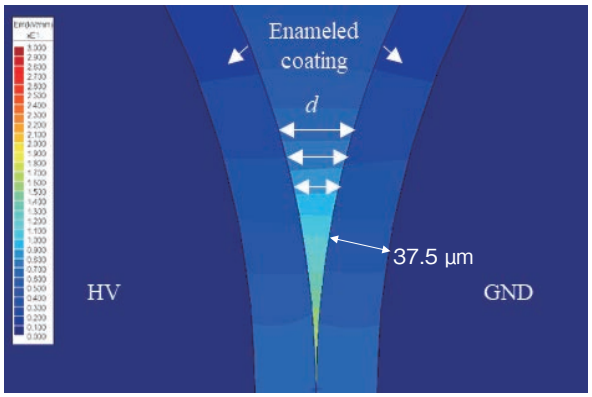

Figure 8 Electric field strength analysis result of the twisted pair wedge.

When E-d curve at a given V_a touches with Paschen's curve of the air at atmospheric pressure (see Figure 9), V_a is taken as estimated PDIV of the specimen, as shown in Figure 9, AC PDIV is determined to be 0.94 kV of the peak value. The relative permittivity and the enameled coating thickness of the cellular sample used for the electric analysis were an actual measured value. And also the PDIV of the non-cellular specimen was estimated using the same method.

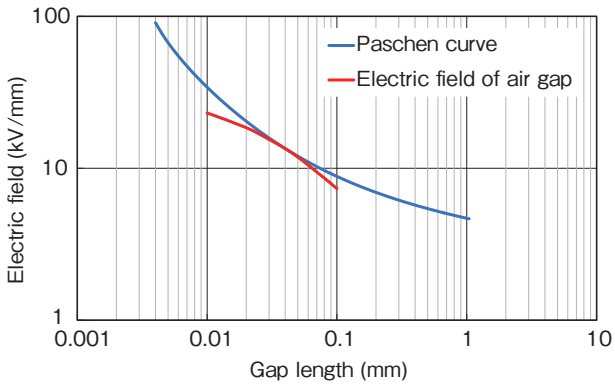

Figure 9 Paschen curve and electric field strength of the wedge gap at 0.94 kV of V_a for the cellular coating twisted pair specimen.

Figure 10 shows the relationship between the measured value and the estimated value. According to Figure 10, the measured value and the estimated value of the PDIV shows the same trend. The result suggests that the decreasing of the PDIV with the increase in the elongation rate is governed by the thinning of the insulation thickness rather than the decreasing of the permittivity with changing of the cellular shape.

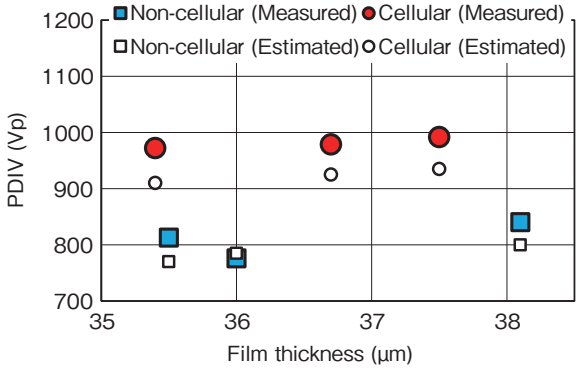

Figure 10 Comparison between the measured value and the estimated value for PDIV.

4. THE INFLUENCE OF APPLYING VOLTAGE WAVE ON THE PDIV OF THE CELLULAR WINDIN WIRE

The surge voltage and the driving power voltage are superimposed on an inverter motor integrated in xEV by high speed switching. The surge voltage is called the inverter surge in general which makes the partial discharge between the winding wires of the driving power motor, and the partial discharge is capable of damaging the insulation coating. It is important to clarify theoretically the partial discharge on the winding wire under the inverter surge.

In order to investigate the partial discharge performance when the steep rising impulse voltage simulating the inverter surge repeatedly applies on the cellular coating, the PDIV performance of the twisted pair wire was evaluated and the result was discussed by Volume-Time theory[4), 5), 6)-9)].

4.1 Experiment Method

4.1.1 Twisted pair specimen

The specimen was Polyamide imide (PAI) containing a lot of micro cellular coating with 3 μm of average diameter insulation twisted pair wire, whose structure is shown in Figure 3, The relative permittivity of the total cellular coating was 2.5. The non-cellular PAI insulation twisted pair wire was prepared for comparison. The conductor diameter and the coating thickness of the specimens were 1.0 mm and 37 μm respectively.

4.1.2 The partial discharge inception voltage (PDIV)

The repetitive impulse voltage was applied on the specimen and the PDIV was evaluated using a measurement circuit shown in Figure 11 (Impulse test). The specimen was placed in the dark box for the impulse test shown in Figure 11, and light emission (PD emission) and electromagnetic wave generated by applying the bipolar impulse voltage were caught by the photomultiplier tube (PMT) (Hamamatsu photonics K.K. H10721-210) and the loop sensor with triggering the PMT signal. The PMT and the loop sensor were placed at a distance 15 cm away from the specimen. In addition, a mirror was placed in the dark box for PMT to catch the PD light emission generated on the back side of the specimen. Bipolar impulses voltage generated by the inverter pulse generator (Pulse Electronics Co., Ltd., PG-W5KE) were used for the impulse test with a rise time of 200 ns, a pulse width of 1 μs, a repetition frequency of 500 Hz, and a voltage rise rate of 500 v / min. The measurement using AC voltage was the same way in the section 3.1.2. Five specimens for each type were used in the AC and impulse test. The number of the PDIV measurement for each specimen was 10. The PDIV was evaluated for the crest value for the AC and for the repetitive impulse voltage.

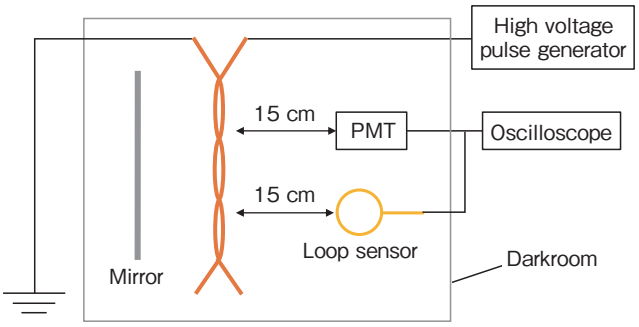

Figure 11 Measurement circuit of partial discharge under repetitive bipolar impulse voltage.

4.2 Experiment Result and Discussion

4.2.1 Partial discharge test for AC and repetitive impulse test

Figure 12 shows the PMT signal, the applied impulse voltage wave and the detected signal with the loop sensor as an example of the partial discharge signal wave at the impulse test for the cellular specimen. The partial discharge pulse occurring during the flat part of an applied impulse voltage is detected with both PMT and loop sensor, while PMT output includes noise occurring at the rise part of an impulse voltage in a switching operation. Figure 13 shows the result of the PDIV measurement in the AC and impulse test for both types of specimens. The result shows that PDIV of the cellular specimen in both AC and impulse voltages are improved by 20 % compared to the non-cellular specimen. The impulse ratio representing the ratio of the repetitive impulse PDIV to the AC PDIV is 1.15 for the non-cellular and 1.14 for the cellular specimen.

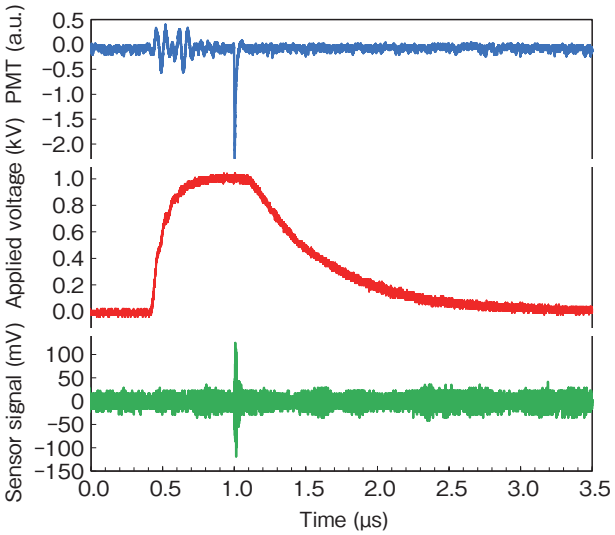

Figure 12 The waveform of PD signal under the impulse voltage.

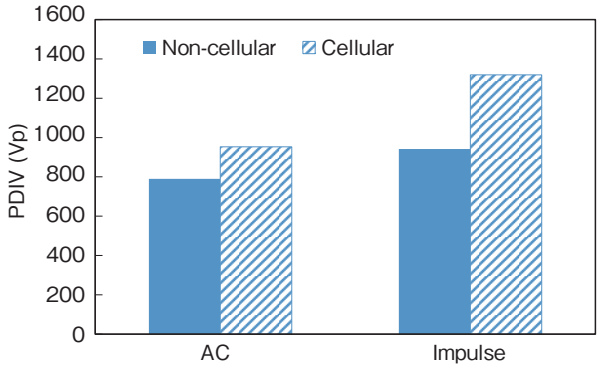

Figure 13 Measured PDIV of non-cellular and cellular coating twisted pair under AC and repetitive impulse voltages.

4.2.2 Estimation of PDIV using volume-time theory

The estimation of both AC and impulse PDIV was performed using Volume-Time theory which considers discharge process in the air wedge gap of the enameled twisted pair under AC and impulse voltage applications, respectively. The volume-Time theory provides generation probability of initial electrons by considering spatial and temporal change of electric field formed in an insulation system. In other words, a generation probability P of initial electrons can be calculated by Volume-Time theory for a given applied voltage wave form to a test electrode system. This calculation assumes electron detachment from negative ions in the air and field electron emission from the surface of the enameled coating on the cathode to supply initial electrons. The generation probability P of initial electrons is given by equation (4)[7)-9)].

$$P = 1 - \exp\left[-\int_0^t \left(\int_{V_{cr}} \frac{dn}{dt} dV + \int_{S_{cr}} \frac{di}{dt} dS \right) dt \right] \quad (4)$$

Where dn/dt and di/dt represent expected generation number value of initial electrons due to electron detachment from negative ions in air and electron emission from the enameled coating surface, respectively. The V_{cr} and S_{cr} in the integration domain of equation (4) are the critical volume and the critical surface respectively.

The generation of initial electrons detached from O_2^- ion is explained. The initial electron numbers detached from O_2^- ions in the air per unit time and volume is given by the product the ion density n^- of O_2^- and detachment coefficient k_d as shown in the following equation (5)[9)].

$$\frac{dn}{dt} = k_d \times n^- \quad (5)$$

Where k_d is the electron detachment coefficient that depends on the overvoltage rate E/E_{cr} defined as the electric field E in the air divided by the critical electric field E_{cr}[8)]. Note that the O_2^- ion density n^- in the air at the atmospheric pressure was defined as 150 ions / cm^3.

Next, the generation of initial electrons by the field electron emission on the enameled coating surface is explained. Generally, electric field electron emission based on Fowler-Nordheim (FN) theory occurs at protrusions on the cathode surface. Recently, it has been clarified that the field electron emission similar to FN theory occurs for the insulator containing impurity or deposits existing on the cathode surface[12)]. Hence, it is considered that the initial electrons are emitted from the impurities, deposits or trap levels of the coating insulation under high electric field. In order to take this phenomenon into the calculation, an equation representing the field electron emission by FN theory was used[13)]. The expected number di/dt of the electrons emitted from the enameled coating surface per unit time and area is expressed by equation (6).

$$\frac{di}{dt} = \frac{e^3 (\beta E_i)^2}{8\pi h (e\phi_D)} \exp\left[-\frac{8\pi\sqrt{2m}}{3he\beta E_i} (e\phi_D)^{\frac{3}{2}} \right] \quad (6)$$

Where e is the electron charge, m is effective electron mass, h is Plank's constant, β is field enhancement factor, ϕ_D is potential barrier height and E_i is electric field of the enameled coating. Since high electric field being occurring due to the protrusion and the impurities of the enameled coating, the electric field E_i of the coating was considered to correct with the field enhancement factor β.

The calculation result of the initial electron numbers of expected value di/dt emitted from the enameled coating based on Equation (5) and (6) is shown in Figure 14. It is clear that a lot of initial electrons are provided from the enameled coating at around 20kV/ mm of E according to the Figure 14. The field electron emission based on FN theory is observed at tens of kV/mm of electric field according to the reference[12)], and it is similar to the above E value.

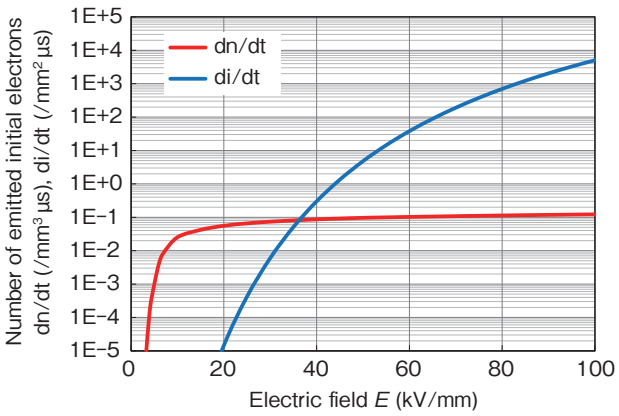

Figure 14 Expected number of emission electrons from the coating surface per unit time and volume (*di/dt*), and expected number of emission electrons from air per unit time and volume (*dn/dt*)

To generate the discharge in the gas, it is needed for the generated initial electron to repeat the impact ionization to grow a streamer (discharge path). Thus the partial

discharge generation probability can be calculated by integrating the initial electron generation probability P over the region V_{cr} where the initial electrons can transit to the streamer. The V_{cr} is defined as the critical volume. The critical volume V_{cr} is defined as gas region satisfying the condition formula of the equation (7) for streamer transition[10), 11)].

$$\int_{\chi}(\alpha-\eta)dx = K \tag{7}$$

Where χ is the electron drift path length, α is the impact ionization coefficient, η is the attachment coefficient and K is the number of impact ionization. The effective ionization coefficient $\alpha-\eta$ in air is given by equation (8) using the electric field E [kV/mm] and the air pressure [MPa]. Note that E has to exceed the critical electric field E_{cr} of 23.86 kV/(mm*MPa) of air.

$$\frac{\alpha-\eta}{p} = 0.186\left(\frac{E}{p}-23.86\right)^2 \tag{8}$$

K is a constant determined by the type of gas, where 10 was used. It is assumed that the electron drift takes a linear trajectory from the ground side to the voltage side, and the calculation was performed by assuming that the electron drift path length χ is equivalent to the gap length d. The surface area of the ground side enameled wire in contact with V_{cr} was defined as the critical surface area S_{cr}.

4.2.3 The calculation result based on volume-time theory and discussion

The calculated partial discharge probability P_{PD} based on equation (4) of the non-cellular specimen depending on the peak value of applied voltage V_i is shown in Figure 15 (a). Figure 15 (b) shows the calculation result of P_{PD} vs. V_i in the case of excluding the initial electron emission from the coating surface (di/dt) in the equation (4).

The calculation result of partial discharge probability P_{PD} for the cellular sample is also shown in Figure 16 (a) and (b). The solid line shows the calculation result under AC voltage in the Figure 15 and Figure 16 and the broken line shows the result under impulse voltage. It is obvious in Figure 15 and Figure 16 that the calculated P_{PD} vs. V_i by equation (4) agrees with the calculation without considering the field electron emission term di/dt under AC voltage application.

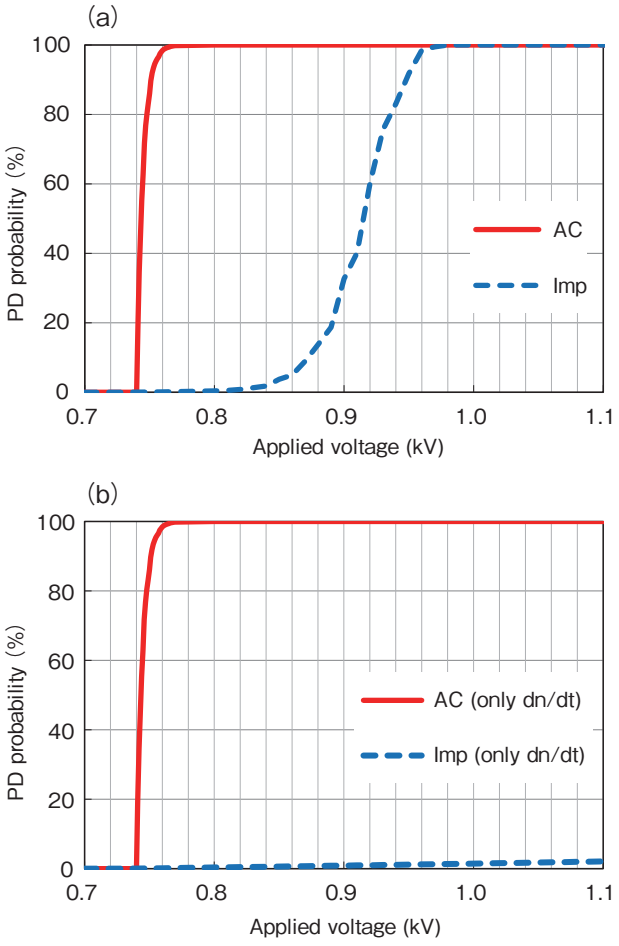

Figure 15 PD probability dependence on the applied voltage for the non-cellular specimen.
(a) Calculated value by equation (4).
(b) Calculated value by equation (4) excluding of the term *di/dt*.

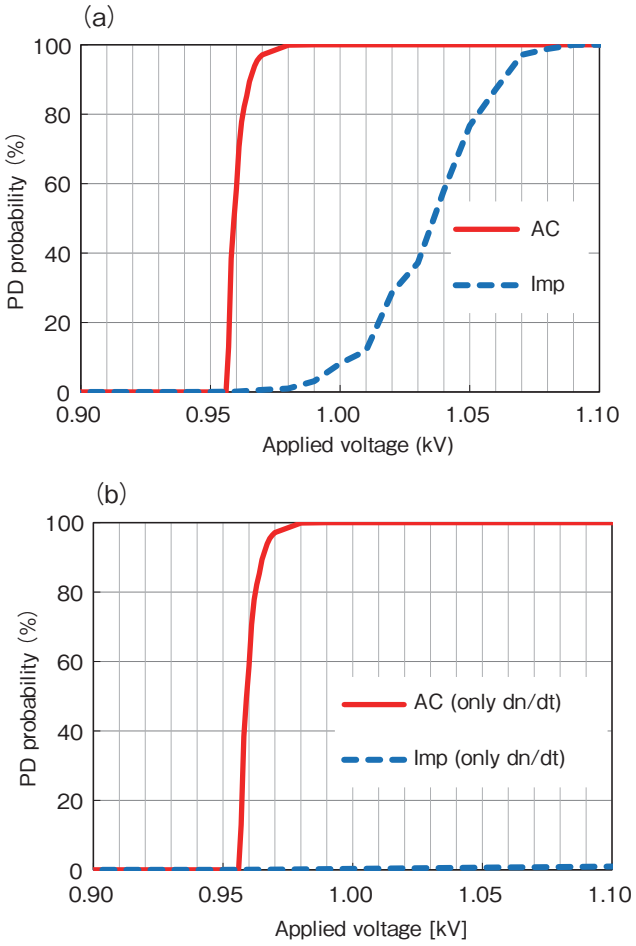

Figure 16 PD probability dependence on the applied voltage for the cellular specimen.
(a) Calculated value by equation (4).
(b) Calculated value by equation (4) excluding of the term *di/dt*.

This indicates that, even for the air gap where a little of initial electron numbers are emitted per unit time (see Figure 14), the initial electrons are sufficiently supplied from the air gap, satisfying with the equation (5), irrespective of the field electron emission from the enameled coating surface under AC voltage application which lasts relatively a long period in the order of several milliseconds.

On the other hand, under impulse voltage, large discrepancy appears between calculated results with and without considering the term *di*/*dt* in equation (4). The discrepancy indicates that the impulse voltage with a pulse width 1 μs is too short to supply the initial electrons from air gap satisfying with equation (5) and lower the probability to generate the discharge, while the field electron emission from the enameled coating surface is dominant in the high electric field (see Figure 14) and supplies the initial electrons to satisfy with equation (5) which leads to higher discharge generation probability.

According to Figure 15 (a) and Figure 16(a), AC and impulse voltage values of the cellular specimen were higher than those of the non-cellular specimen. This result suggests that the permittivity of the cellular specimen is lower than that of the non-cellular specimen, and the lower permittivity affects the electric field E_i of equation (8), which leads the initial electron generation from the enamel coating to be suppressed.

Next, according to Figure 15 (a) and Figure 16 (a), calculated PDIV derived from P_{PD} was compared with measured PDIV. It is assumed that the calculated PDIV is determined when the number of initial electrons generated within the critical volume V_{cr} equals 1: i.e. corresponding to P_{PD} = 63.2 %. Figure 17 (a) and (b) show measured ($PDIM_{Me}$) and calculated PDIV by Volume-Time theory ($PDIV_{VT}$) as well as by Paschen's law ($PDIV_{Ph}$) of the wedge gap for the non-cellular and cellular specimens under each voltage waveform, respectively. It can be seen in these figures that a good agreement is obtained among the $PDIM_{Me}$, $PDIV_{VT}$, $PDIV_{Ph}$ for both types of specimens. Besides, calculated impulse PDIV by Volume-Time theory ($PDIV_{VT}$) agrees well with measured one ($PDIM_{Me}$). Thus, it is suggested that Volume-Time theory provides reasonable solution of PDIV under both AC and impulse voltage applications. The cellular specimen has a higher PDIV than the non-cellular specimen due to lowering permittivity.

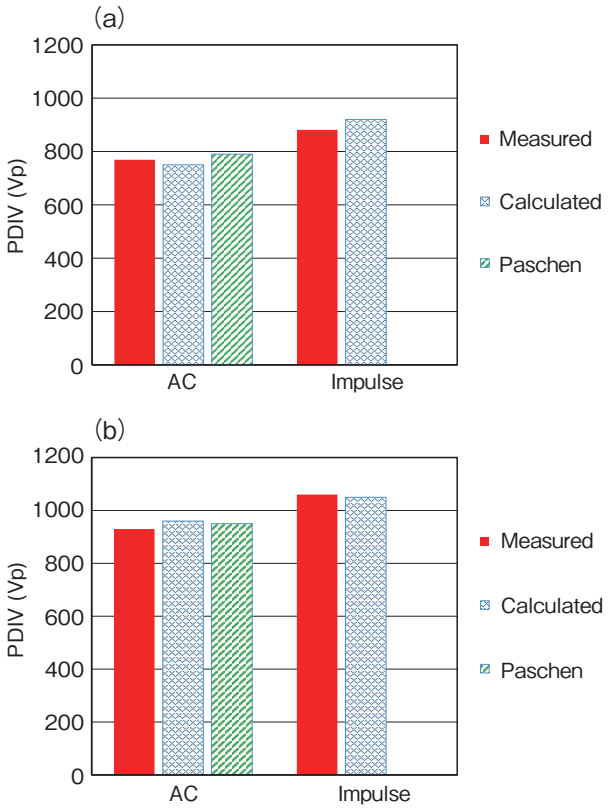

Figure 17 Comparison of measured PDIV and calculated PDIV. (a) Non-cellular specimen. (b) Cellular specimen.

The above calculation result suggests that most of initial electrons which occur in the partial discharge under the impulse voltage are the electron emitted from the enamaled coating surface.

5. CONCLUSION

We investigated the influence of the mechanical stress and the applied voltage on the partial discharge performance for the winding wire utilizing the micro cellular enameled coating, on the assumption that the cellular wire is integrated in the inverter of the driving motor. The result is shown below:

- The PDIV value of the cellular specimen was 18% to 26% higher than that of the non-cellular specimen at the elongation rates of 10% to 30%.
- The cause of the PDIV decreasing with the increase of elongation rate is due to the decrease of the cellular enameled coating thickness.
- The relative permittivity of the cellular enameled wire was decreasing with the increase of the elongation rate.
- The PDIV of the cellular specimen was increased around 20% more than that of the non-cellular specimen under AC and repetitive impulse voltage applications.
- The ratio of the PDIV under AC voltage application to the PDIV under repetitive impulse voltage is 1.15 for the non-cellular specimen and 1.14 for the cellular specimen respectively.
- The measured PDIV value under the AC voltage and the repetitive impulse voltage application are in a good agreement with the estimated value by the Volume-Time theory.

According to the above results, the cellular enameled coting wire maintained excellent performance after the elongation or the repetitive impulse voltage applications, this result suggests that the cellular wire is adequate. Furthermore the estimation of the PDIV using the Volume-time theory is useful as a theoretical solution method for the PDIV under AC and impulse voltages.

Since the motors integrating cars are requiring more size reduction and higher performance, this report can contribute to further innovation on motor designs. We continue to focus on the low permittivity material and the eddy current loss of motors and to develop materials for improving the motor performance.

ACKNOWLEDGEMENT

We would like to express our appreciation to Mr. Tomohiro Kubo of Master course and Mr. Kenta Maeda of Master course of Kyushu Institute of Technology for their cooperation in the data acquisition and in the discussion on this study.

REFERENCES

1) Muto, Ohya, Aoi and Ueno, “A Study on Partial Discharge Phenomena of Winding Wires”, Furukawa Review No.45 (2014) pp. 13-21
2) Tomizawa, Shimada, Ikeda, Muto and Fukuda, “The Development of Next-Generation Technologies in the Domain of Winding Wires of Main Electric Motors”, Furukawa Electric Review, No. 49 (2018) pp. 9-15
3) Kubo, Nakano, Kozako, Hikita, Fukuda, Ikeda, Tomizawa and Muto, “The dielectric and partial discharge performance of the elongated micro cellular enameled coating wire” 49th Electrical and electronics insulation material system symposium, D2 (2018) 123-126 (in Japanese)
4) Maeda, Kubo, Uchimura, Mizoguchi, Kozako, Hikita, Fukuda, Muto, Tomizawa and Ikeda, “Estimation of the impulse partial discharge inception voltage for the cellular coating twisted pair wire using Volume-Time theory” Discharge / dielectric · insulation material / high voltage united study group, ED-18-002, HV-18-042 (2018) 7-12 (in Japanese)
5) K. Maeda, T. Kubo, T. Uchimura, H. Mizoguchi, M. Kozako,M. Hikita, H. Fukuda, D. Mutou, K. Tomizawa, K. Ikeda,“Partial Discharge Inception Voltage of Enameled Cellular Wire under Impulse Voltage”, 2ND IEEE INTERNATIONAL CONFERENCE ON DIELECTRICS, No.3 (2018).
6) X. Xu, S. Jayaram, S. A. Boggs,“ Prediction of Breakdown in SF6 under Impulse Conditions”, IEEE Transactions on Dielectrics and Electrical Insulation, 3, No.6 (1996),836-842.
7) K. Maeda, S. Nakamura, M. Kozako, M. Hikita, S. Yoshida, T. Chigiri, “Partial Discharge Characteristics of Wedge-Shaped Gap between Coated Electrodes in SF6 under Lightning Impulse Voltage”, 21th International Conference on Gas Discharge and their Applications, 1 (2016), 301-304.
8) K. Maeda, M. Kozako, M. Hikita, S. Yoshida, T. Chigiri,“Partial Discharge Inception Voltage Measurement and Its Estimation by Volume-Time Theory for SF6/PET Insulated Wedge Gap under Impulse Voltage”, 20th International Symposium on High Voltage Engineering, No.441 (2017).
9) N. Hayakawa, F. Shimizu, H. Okubo, “Estimation of Partial Discharge Inception Voltage of Magnet Wires under Inverter Surge Voltage by Volume-Time Theory”, IEEE Transactions on Dielectrics and Electrical Insulation, 19, No.2 (2012), 550-557.
10) IEE Japan discharge handbook publication committee ed., “Discharge Handbook”, Ohm Corporation, Japan, pp. 516-521 (1998) (in Japanese)
11) H. Okubo ed. “High Electric Field Phenomenology” Ohm Corporation, pp. 85-94 (2011) (in Japanese)
12) IEE Japan discharge handbook publication committee ed. , “Discharge Handbook”, Ohm Corporation, Japan, pp. 598-604 (1998) (in Japanese)
13) H. Okubo ed. “High Electric Field Phenomenology” Ohm Corporation, pp. 74-75 (2011) (in Japanese)